Determination of Protein Structures in the Solid State from NMR Chemical Shifts

Paul Robustelli,[1] Andrea Cavalli,[1] and Michele Vendruscolo[1],*

[1]Department of Chemistry, University of Cambridge, Lensfield Road, Cambridge CB2 1EW, UK

*Correspondence: mv245@cam.ac.uk

DOI 10.1016/j.str.2008.10.016

SUMMARY

Solid-state NMR spectroscopy does not require proteins to form crystalline or soluble samples and can thus be applied under a variety of conditions, including precipitates, gels, and microcrystals. It has recently been shown that NMR chemical shifts can be used to determine the structures of the native states of proteins in solution. By considering the cases of two proteins, GB1 and SH3, we provide an initial demonstration here that this type of approach can be extended to the use of solid-state NMR chemical shifts to obtain protein structures in the solid state without the need for measuring interatomic distances.

INTRODUCTION

Solid-state nuclear magnetic resonance (SSNMR) spectroscopy can be applied under a variety of conditions not accessible to X-ray crystallography and solution NMR (Griffin, 1998; McDermott, 2004; Opella and Marassi, 2004; Hologne et al., 2006; Baldus, 2007; Brown, 2007). In recent years, crucial advances have enabled the detection of carbon-nitrogen, carbon-carbon, and proton-proton distances in the solid state, and the first structures of proteins determined by SSNMR have appeared (Castellani et al., 2002; Lange et al., 2005; Zech et al., 2005; Zhou et al., 2007a). SSNMR structure calculations have not yet become routine, however, due to the experimental, methodological, and instrumental difficulties involved in obtaining the necessary spectral resolution and sensitivity required for the measurement of a sufficient number of unambiguous interatomic distance restraints. In an effort to further increase the scope of SSNMR in structural biology, we provide initial evidence here that it is possible to use solid-state chemical shifts as the sole source of experimental information for protein structure calculations, without the use of interatomic distance restraints.

Although chemical shifts are the most readily and accurately measurable NMR observables, the development of methods that use chemical shifts for structure determination has been challenging because the chemical shift associated with a specific atom is a summation of many contributing factors (Xu and Case, 2001; Neal et al., 2003; Shen and Bax, 2007). This complex set of dependencies makes it very difficult to reliably identify interaction partners from chemical shifts, even though they may be substantially influenced by contacts such as hydrogen bonding and proximity to aromatic rings between residues that are at very different

locations in the protein sequence. Despite these problems, much progress has been made in the use of structural information provided by chemical shifts to aid the determination of native-state conformations of proteins (Williamson and Asakura, 1993; Kuszewski et al., 1995; Luginbuhl et al., 1995; Pearson et al., 1995; Wilton et al., 2008). Recent approaches including CHESHIRE (Cavalli et al., 2007; Montalvao et al., 2008), CS-Rosetta (Shen et al., 2008), and CS23D (Wishart et al., 2008) have shown that backbone chemical shifts measured in solution can be used to solve protein structures of up to 130 residues representative of the major structural classes to a resolution of 2 Å or better.

Because there are significant and nonsystematic differences between chemical shifts measured for molecular systems in the solid state and in solution (van Rossum et al., 2001, 2003; Franks et al., 2005; Zhou et al., 2007b), in this work we investigated whether the CHESHIRE protocol is applicable for chemical shifts measured by SSNMR. We first considered a protein whose native-state structure is well characterized both in solid-state and solution environments (Gronenborn et al., 1991; Kuszewski et al., 1999; Ulmer et al., 2003; Franks et al., 2006; Schmidt et al., 2007; Zhou et al., 2007a), the β1 immunoglobulin binding domain of protein G (GB1). The differences in the GB1 chemical shifts in the solid state and in solution are shown in Figure 1 (Franks et al., 2005; Zhou et al., 2007a, 2007b). In this work, we utilized Cα, Cβ, Hα, and N chemical shifts measured by proton-detected magic-angle-spinning SSNMR (MAS-SSNMR) (Franks et al., 2005; Zhou et al., 2007a, 2007b); in many cases, the differences in the chemical shifts of these atoms in the solid state and in solution are larger than the accuracy in the estimates of the chemical shifts themselves, provided by current prediction methods (Xu and Case, 2001; Neal et al., 2003; Shen and Bax, 2007). The results that we present indicate that the application of the CHESHIRE approach to GB1, which was originally developed for solution NMR data (Cavalli et al., 2007), results in an accurate structure despite the effects the microcrystalline environment has on the chemical shifts.

CHESHIRE, the method used in this investigation, consists of a three-phase computational procedure (Cavalli et al., 2007). In the first phase, the chemical shifts and the intrinsic secondary structure propensities of amino acid triplets are used to predict the secondary structure of the protein. In the second phase, the secondary structure predictions and the chemical shifts are used to predict backbone torsion angles for the protein. These angles are screened against a database to create a library of trial conformations of three and nine residue fragments spanning the sequence of the protein. In the third phase, a molecular fragment replacement strategy is used to bring together these fragments into low-resolution structural models; the information provided
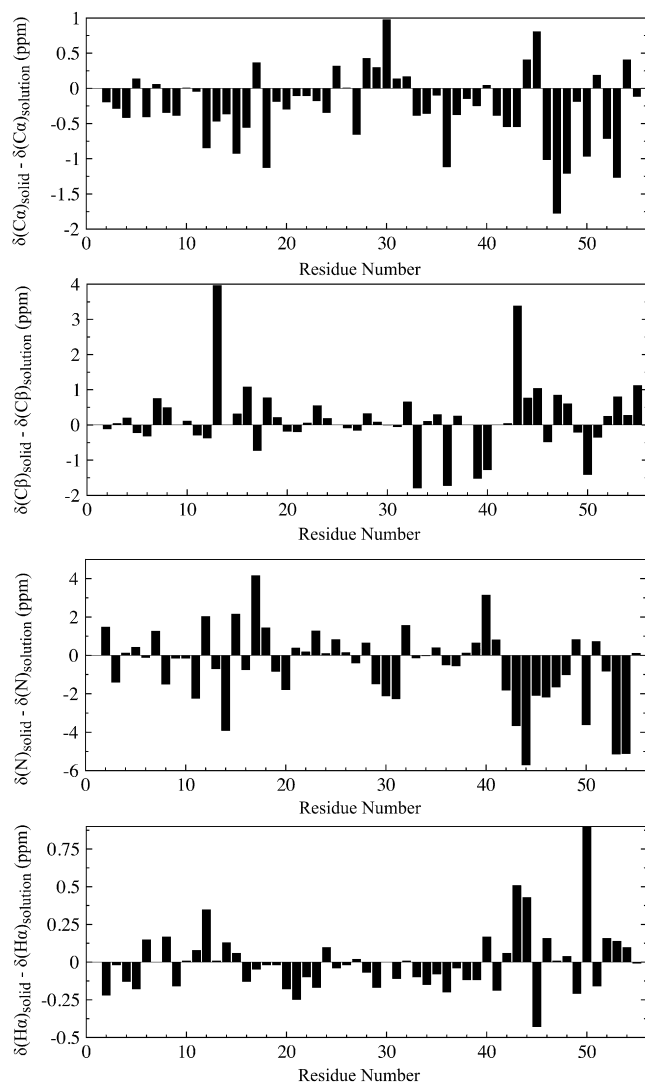
Figure 1. Analysis of the Differences between Solution and Solid-State Chemical Shifts

Comparison of the Cα, Cβ, N, and Hα chemical shifts of GB1 used in this work in the solid state and in solution (van Rossum et al., 2001, 2003; Franks et al., 2005; Zhou et al., 2007b).

by chemical shifts is used in this phase to guide the assembly of the fragments. The resulting structures are refined with a hybrid molecular dynamics and Monte Carlo conformational search using a scoring function defined by the agreement between the experimental and calculated chemical shifts and the energy of a molecular mechanics force field, ensuring that a structure will obtain a low CHESHIRE score only if it has a low value of the molecular mechanics energy and a very close agreement with experimental chemical shifts. The three phases of the CHESHIRE protocol are described in more detail below.

Phase 1: Chemical Shift-Based Prediction of Secondary Structure Propensities

In the first step of the CHESHIRE procedure, chemical shifts are used to predict the propensities for secondary structure forma-

tion. We used the 3PRED method (Cavalli et al., 2007), which uses Bayesian inference to predict the secondary structure of amino acids from the knowledge of the chemical shifts in combination with the intrinsic secondary structure propensity of amino acids. The latter propensities were computed by considering all the structures in the ASTRAL SCOP database (Chandonia et al., 2002) having less than 25% sequence identity according to the secondary structure classification provided by the program STRIDE (Frishman and Argos, 1995). Chemical shifts for the proteins in this database were calculated by applying SHIFTX (Neal et al., 2003) in order to obtain an extensive database (3PRED-DB) which consisted of 939,639 calculated chemical shifts for each atom type (Cavalli et al., 2007).

Phase 2a: Chemical Shift-Based Prediction of Dihedral Angle Restraints

In the second step of the CHESHIRE procedure, the secondary structure propensities computed by 3PRED are used as input in TOPOS (Cavalli et al., 2007), an algorithm based on an approach similar to that of TALOS (Cornilescu et al., 1999), to predict the backbone torsion angles that are most compatible with the experimental chemical shifts. In TOPOS, for each protein segment of three residues in the sequence (the target), the similarity to a triplet in a sequence in the ASTRAL SCOP database (the source) is evaluated. To avoid overfitting problems due to the use of a limited database, TOPOS uses the same extensive database of 3PRED. In each individual case, we remove all sequences with a sequence similarity larger than 10^{-3} (Cavalli et al., 2007). The fragments with the highest scores are then clustered together according to the distance of the backbone torsion angles of the central amino acid. Finally, the average dihedral ϕ and ψ angles for the three best-scoring clusters are reported as prediction (Cavalli et al., 2007).

Phase 2b: Prediction of the Structures of Fragments

The CHESHIRE method is based on the molecular fragment replacement approach, which has been shown to be successful for the determination of protein structures with residual dipolar couplings (Delaglio et al., 2000) and in ab initio structure determination (Schueler-Furman et al., 2005). In the CHESHIRE method, two types of fragments, of three and nine amino acids, are selected from the ASTRAL SCOP Protein Data Bank (PDB) database. The scoring function takes into account three contributions: (1) the score between the experimental chemical shifts of the fragment of the protein considered and the chemical shifts of the structure in the database; (2) the score for the compatibility with the dihedral angle restraints obtained with TOPOS; and (3) the score for the match between the predicted secondary structure and the secondary structure of the fragment.

Phase 3a: Generation of Low-Resolution Structures

In the initial low-resolution structure generation, a coarse-grained representation of the protein chain is used in which only backbone atoms are explicitly modeled; side chains are represented by a single C_β atom. Bond lengths, angles, and the ω backbone torsion angle are kept fixed, while ϕ and ψ torsion are given the freedom to move. The energy function used for the generation of low-resolution structures is a linear combination of terms that model the features of folded proteins. van
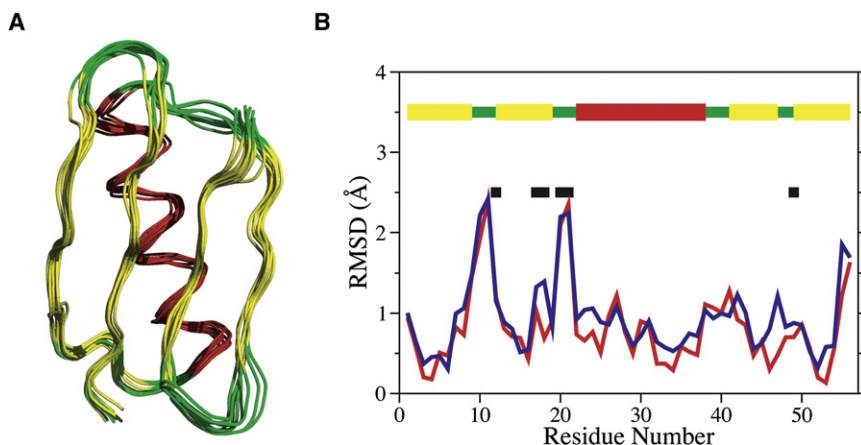
A

B

der Waals and electrostatic forces are adapted from CHARMM PARAM19 (Brooks et al., 1983) and solvation is treated according to Lazaridis and Karplus (1999). In addition, a pairwise potential of mean force is implemented using all known PDB structures in the ASTRAL SCOP database following Zhou and Zhou (2002). In order to correctly model the packing of secondary structure elements, the potential of Baker and coworkers (Simons et al., 1999) was implemented. Low-resolution structures were generated using a Monte Carlo algorithm carried out in an extended configuration space given by the cartesian product of the protein chain coordinates and a "virtual secondary structure" string (Cavalli et al., 2007). Starting from a fully extended chain, conformations are generated by 20,000 Monte Carlo moves using a simulated annealing protocol. Two kinds of moves are applied. In the first (fragment substitution), the torsion angles and the secondary structure string in a randomly selected three or nine residue window of the protein chain are replaced with those from a fragment of known structure. In the second, local backbone moves, the torsion angles, but not the secondary structure, of a window of four amino acids are randomly perturbed. The score of the new conformation is calculated and the move is accepted according to the Metropolis criterion. For each of the proteins studied here, 10,000 trial structures were generated in this way.

Phase 3b: Generation of High-Resolution Structures
In this phase, all atoms are represented explicitly from the trial structures generated from the previous low-resolution stage (Cavalli et al., 2007). In a first stage, bond lengths, angles, and the ω backbone torsion angles are kept fixed, while the ϕ, ψ, and side-chain torsion angles are let free to move. Structures are then optimized using the CHESHIRE energy function (described below). Finally, the best-scoring structures are further refined by repeated minimizations and side-chain optimizations using the Dunbrack and Cohen rotamers library (Dunbrack and Cohen, 1997). Initial structures are obtained by adding the missing atoms to the low-resolution structures using the following protocol. (1) A fully extended all-atom protein chain is generated using ideal geometries. (2) Target ϕ and ψ angles are set to those of the source chain. (3) An energy minimization of 10,000 steps is performed to remove steric clashes. (4) An additional energy minimization of 10,000 steps is performed by restraining interbackbone distances to the original ones. (5) A final energy mini-

mization of 10,000 steps is performed without any restraint. After the addition of the side-chain atoms, the scores of all structures are computed according to the CHESHIRE energy function, a combination of a physicochemical term and a term that describes the correlation between experimental and predicted chemical shifts, and the best 500 structures are selected for refinement.

The refinement consisted of a simulated annealing Monte Carlo run of 10,000 steps, where each Monte Carlo move consists of a short run of unrestrained molecular dynamics. The use of the hybrid molecular dynamics and Monte Carlo conformational search strategy enables us to use a bias on the chemical shifts without requiring the derivatives of the cost function, as would be necessary in a restrained molecular dynamics scheme. After refinement, structures are ranked according to their scores and the best-scoring one is selected as the final result (Cavalli et al., 2007).

Determination of the Structure of GB1
The lowest-energy structure of GB1 solved from Cα, Cβ, Hα, and N solid-state NMR chemical shifts (PDB ID code 2K0P) is characterized by correlation coefficients between observed and calculated chemical shifts of 0.961 (Cα), 0.995 (Cβ), 0.737 (N), and 0.915 (Hα). These accuracies are comparable to the resolution of SHIFTX (Neal et al., 2003), the chemical shift predictor used in CHESHIRE. The 2K0P structure has a root-mean-square deviation (rmsd) from a crystal structure (PDB ID code 2GI9) (Franks et al., 2006) of 0.93 Å for the backbone and 1.70 Å for all heavy atoms (Figure 2; Table 1). The rmsd per residue is shown by a red line in Figure 2B, which illustrates that the differences in the conformations are localized in turns and loops, whereas they are significantly smaller within secondary structure elements.

The quality of the structure determined here from solid-state chemical shifts can be assessed by a comparison with other structures of the same protein determined from X-ray crystallography and solution NMR methods (Table 1). We considered the Q factors for residual dipolar couplings (RDC) (Bax et al., 2001) and the number, N, of interproton distances below 5.5 Å in the X-ray structure and above 6.5 Å in the query structure. According to these structural descriptors, the RDC-refined X-ray structure 1P7F (Ulmer et al., 2003) is the closest structure to the crystal structure 2GI9, followed by the solution NMR structures 3GB1 (Kuszewski et al., 1999) and 2GB1 (Gronenborn et al., 1991). The

Table 1. Comparison of the Structure of GB1 Derived from Chemical Shifts with Those Determined by Standard Approaches

Structure	Rmsd	N	Q
1P7F	0.40	0	0.03
3GB1	0.59	0	0.16
2GB1	0.97	1	0.37
2JU6	1.86	5	0.48
2JSV	1.57	4	0.37
2K0P	0.93	2	0.35

The lowest-energy structure determined using chemical shifts (PDB ID code 2K0P) is compared with an RDC-refined X-ray structure (PDB ID code 1P7F) (Ulmer et al., 2003), a solution NMR structure (PDB ID code 3GB1) (Kuszewski et al., 1999), another solution NMR structure (PDB ID code 2GB1) (Gronenborn et al., 1991), a solid-state NMR structure derived from interatomic distances (PDB ID code 2JU6) (Zhou et al., 2007a), and a solid-state NMR structure derived from interatomic distances and dipole tensor refinement (PDB ID code 2JSV) (Franks et al., 2008). Rmsd, backbone root-mean-square deviation from the crystal structure 2GI9 (Franks et al., 2006); N, number of interproton distances below 5.5 Å in the X-ray structure and above 6.5 Å in the query structure; Q, quality factor for RDCs (Bax et al., 2001) determined using the five sets of RDCs measured in different alignment media deposited with 1P7F.

solid-state NMR structures 2JU6 (Zhou et al., 2007a), which was derived from proton-proton interatomic distances and TALOS (Cornilescu et al., 1999) restraints, and 2JSV (Franks et al., 2008), which was derived with a larger set of interatomic distances and refined with dipole tensors, exhibit slightly more interproton distance violations and higher Q factors than the 2K0P structure.

The use of chemical shift restraints enables the determination of a well-defined conformation, because the combination of the chemical shift score and the force field that we have used results in a funneled energy landscape (Figure 3). The lowest-energy structures that we have determined are close to the crystal structure 2GI9, and structures that are significantly different have much higher energies.
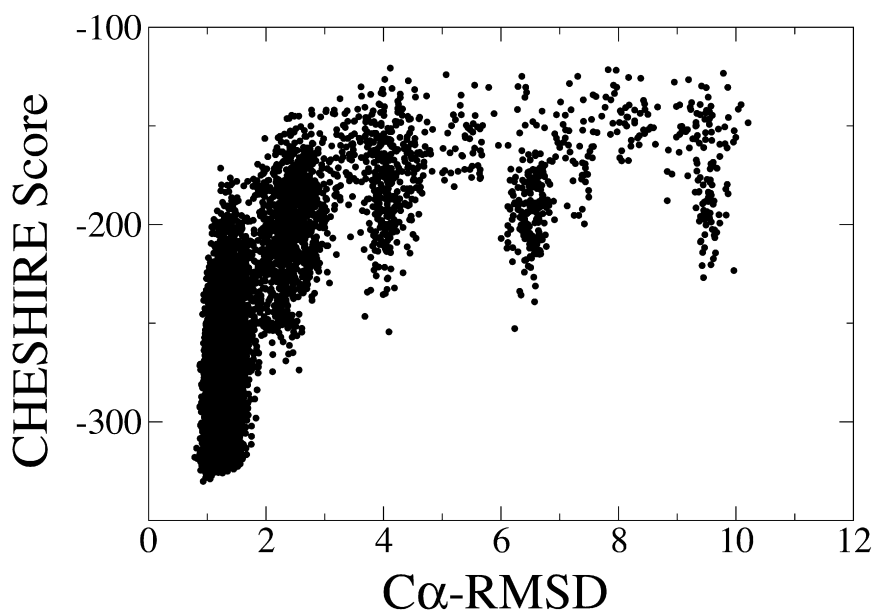
In order to further assess the amount of structural information provided by chemical shifts, we considered the ensemble of the ten structures of lowest CHESHIRE score (Figure 2A). The structures having the best scores make up a narrow ensemble characterized by an overall pairwise rmsd of about 0.8 Å. For comparison, we report the positions at which chemical shift differences have been observed in a recent study in different crystal morphologies of GB1 (Schmidt et al., 2007) (Figure 2B). The majority of the differences are found in the β1-β2 and β2-β3 loops, which are also the regions where the largest differences are localized in the ensemble considered here. These results indicate that the type of variability allowed by the chemical shift information is consistent with a higher tendency to change conformation in different crystal forms.

Determination of the Structure of Src SH3

To further test the applicability of CHESHIRE to chemical shifts measured by SSNMR, we also calculated the structure of the α-spectrin Src-homology 3 (SH3) domain from proton-detected MAS-SSNMR chemical shifts (van Rossum et al., 2001, 2003). The structure calculated (Figure 4) has correlation coefficients between observed and calculated chemical shifts of 0.911 (Cα), 0.984 (Cβ), 0.717 (N), and 0.900 (Hα) and a backbone rmsd of 1.38 Å from the previously determined crystal structure (PDB ID code 1SHG) (Musacchio et al., 1992).

Conclusions

In summary, we have demonstrated that it is possible to determine the structures of GB1 and SH3 at relatively high resolutions using solid-state NMR chemical shifts without the need for measuring interatomic distances, despite the effects of the microcrystalline environment on the chemical shifts. Indeed, for each chemical shift type used in this investigation, there are several regions of GB1 and SH3 in which the solid-state and the solution chemical shifts exhibit sizeable differences (Figure 1) (van Rossum et al., 2001, 2003; Franks et al., 2005; Zhou et al., 2007b).
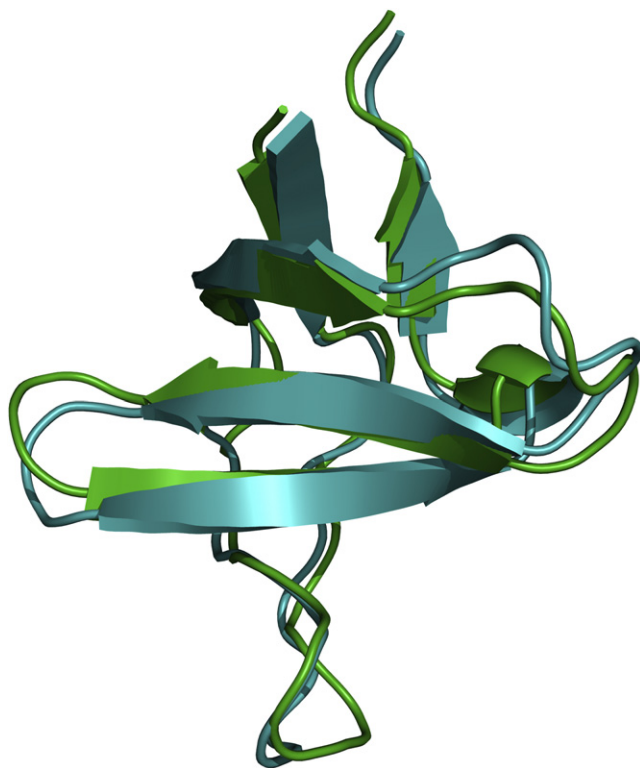

Figure 3. Analysis of the Convergence of the Structure Determination Procedure

Landscape of the CHESHIRE scores of the GB1 structures generated in this work as a function of the rmsd from the GB1 crystal structure 2GI9. The landscape is funneled toward the native structure.

REFERENCES

Baldus, M. (2007). ICMRBS founder's medal 2006: biological solid-state NMR, methods and applications. J. Biomol. NMR *39*, 73–86.

Bax, A., Kontaxis, G., and Tjandra, N. (2001). Dipolar couplings in macromolecular structure determination. Methods Enzymol. *339*, 127–174.

Brooks, B.R., Bruccoleri, R.E., Olafson, B.D., States, D.J., Swaminathan, S., and Karplus, M. (1983). CHARMM—a program for macromolecular energy, minimization, and dynamics calculations. J. Comput. Chem. *4*, 187–217.

Brown, S.P. (2007). Probing proton-proton proximities in the solid state. Prog. Nucl. Magn. Reson. Spectrosc. *50*, 199–251.

Castellani, F., van Rossum, B., Diehl, A., Schubert, M., Rehbein, K., and Oschkinat, H. (2002). Structure of a protein determined by solid-state magic-angle-spinning NMR spectroscopy. Nature *420*, 98–102.

Cavalli, A., Salvatella, X., Dobson, C.M., and Vendruscolo, M. (2007). Protein structure determination from NMR chemical shifts. Proc. Natl. Acad. Sci. USA *104*, 9615–9620.

Chandonia, J.M., Walker, N.S., Conte, L.L., Koehl, P., Levitt, M., and Brenner, S.E. (2002). ASTRAL compendium enhancements. Nucleic Acids Res. *30*, 260–263.

Cornilescu, G., Delaglio, F., and Bax, A. (1999). Protein backbone angle restraints from searching a database for chemical shift and sequence homology. J. Biomol. NMR *13*, 289–302.

Delaglio, F., Kontaxis, G., and Bax, A. (2000). Protein structure determination using molecular fragment replacement and NMR dipolar couplings. J. Am. Chem. Soc. *122*, 2142–2143.

Dunbrack, R.L., and Cohen, F.E. (1997). Bayesian statistical analysis of protein side-chain rotamer preferences. Protein Sci. *6*, 1661–1681.

Franks, W.T., Zhou, D.H., Wylie, B.J., Money, B.G., Graesser, D.T., Frericks, H.L., Sahota, G., and Rienstra, C.M. (2005). Magic-angle spinning solid-state NMR spectroscopy of the β 1 immunoglobulin binding domain of protein G (GB1): ^{15}N and ^{13}C chemical shift assignments and conformational analysis. J. Am. Chem. Soc. *127*, 12291–12305.

Franks, W.T., Wylie, B.J., Stellfox, S.A., and Rienstra, C.M. (2006). Backbone conformational constraints in a microcrystalline U-^{15}N-labeled protein by 3D dipolar-shift solid-state NMR spectroscopy. J. Am. Chem. Soc. *128*, 3154–3155.

Franks, W.T., Wylie, B.J., Schmidt, H.L.F., Nieuwkoop, A.J., Mayrhofer, R.M., Shah, G.J., Graesser, D.T., and Rienstra, C.M. (2008). Dipole tensor-based atomic-resolution structure determination of a nanocrystalline protein by solid-state NMR. Proc. Natl. Acad. Sci. USA *105*, 4621–4626.

Frishman, D., and Argos, P. (1995). Knowledge-based protein secondary structure assignment. Proteins *23*, 566–579.

Griffin, R.G. (1998). Dipolar recoupling in mas spectra of biological solids. Nat. Struct. Biol. *5*, 508–512.

Gronenborn, A.M., Filpula, D.R., Essig, N.Z., Achari, A., Whitlow, M., Wingfield, P.T., and Clore, G.M. (1991). A novel, highly stable fold of the immunoglobulin binding domain of streptococcal protein G. Science *253*, 657–661.

Hologne, M., Chevelkov, V., and Reif, B. (2006). Deuterated peptides and proteins in MAS solid-state NMR. Prog. Nucl. Magn. Reson. Spectrosc. *48*, 211–232.

Kuszewski, J., Gronenborn, A.M., and Clore, G.M. (1995). The impact of direct refinement against proton chemical-shifts on protein-structure determination by NMR. J. Magn. Reson. B *107*, 293–297.

Kuszewski, J., Gronenborn, A.M., and Clore, G.M. (1999). Improving the packing and accuracy of NMR structures with a pseudopotential for the radius of gyration. J. Am. Chem. Soc. *121*, 2337–2338.

Lange, A., Becker, S., Seidel, K., Giller, K., Pongs, O., and Baldus, M. (2005). A concept for rapid protein-structure determination by solid-state NMR spectroscopy. Angew. Chem. Int. Ed. Engl. *44*, 2089–2092.

Lazaridis, T., and Karplus, M. (1999). Effective energy function for proteins in solution. Proteins *35*, 133–152.

Figure 4. Structure of SH3 Determined from Solid-State NMR Chemical Shifts

Comparison of the lowest-energy SH3 structure determined in this work using SSNMR chemical shifts (blue) and a previously determined X-ray structure (PDB ID code 1SHG; green). The structure determined from chemical shifts has an rmsd of 1.38 Å for the backbone atoms.

Our results suggest that despite these differences, the fundamental structural information provided by backbone chemical shifts is captured by the CHESHIRE protocol, even though the latter was developed using chemical shifts measured in solution. As solid-state chemical shifts can be measured for a number of challenging insoluble and noncrystalline structural classes, including membrane proteins, macromolecular complexes, and amyloid fibrils, further progress on the use of structure determination protocols based on chemical shifts, either on their own as shown here or in combination with other NMR observables, may enable a quantitative structural analysis to be carried out for a range of biological problems currently not readily accessible to standard structural techniques.

Luginbuhl, P., Szyperski, T., and Wuthrich, K. (1995). Statistical basis for the use of ^{13}C-α chemical-shifts in protein-structure determination. J. Magn. Reson. B 109, 229–233.

McDermott, A.E. (2004). Structural and dynamic studies of proteins by solid-state NMR spectroscopy: rapid movement forward. Curr. Opin. Struct. Biol. 14, 554–561.

Montalvao, R.W., Cavalli, A., Salvatella, X., and Blundell, T.L. (2008). Structure determination of protein-protein complexes using NMR chemical shifts: case of an endonuclease colicin-immunity protein complex. J. Am. Chem. Soc. 130, 15990–15996.

Musacchio, A., Noble, M., Pauptit, R., Wierenga, R., and Saraste, M. (1992). Crystal-structure of a Src-homology-3 (SH3) domain. Nature 359, 851–855.

Neal, S., Nip, A.M., Zhang, H.Y., and Wishart, D.S. (2003). Rapid and accurate calculation of protein ^{1}H, ^{13}C and ^{15}N chemical shifts. J. Biomol. NMR 26, 215–240.

Opella, S.J., and Marassi, F.M. (2004). Structure determination of membrane proteins by NMR spectroscopy. Chem. Rev. 104, 3587–3606.

Pearson, J.G., Wang, J.F., Markley, J.L., Le, H.B., and Oldfield, E. (1995). Protein-structure refinement using ^{13}C nuclear-magnetic-resonance spectroscopic chemical-shifts and quantum-chemistry. J. Am. Chem. Soc. 117, 8823–8829.

Schmidt, H.L.F., Sperling, L.J., Gao, Y.G., Wylie, B.J., Boettcher, J.M., Wilson, S.R., and Rienstra, C.A. (2007). Crystal polymorphism of protein GB1 examined by solid-state NMR spectroscopy and X-ray diffraction. J. Phys. Chem. B 111, 14362–14369.

Schueler-Furman, O., Wang, C., Bradley, P., Misura, K., and Baker, D. (2005). Progress on modeling of protein structures and interactions. Science 310, 638–642.

Shen, Y., and Bax, A. (2007). Protein backbone chemical shifts predicted from searching a database for torsion angle and sequence homology. J. Biomol. NMR 38, 289–302.

Shen, Y., Lange, O., Delaglio, F., Rossi, P., Aramini, J.M., Liu, G.H., Eletsky, A., Wu, Y.B., Singarapu, K.K., Lemak, A., et al. (2008). Consistent blind protein structure generation from NMR chemical shift data. Proc. Natl. Acad. Sci. USA 105, 4685–4690.

Simons, K.T., Ruczinski, I., Kooperberg, C., Fox, B.A., Bystroff, C., and Baker, D. (1999). Improved recognition of native-like protein structures using a combination of sequence-dependent and sequence-independent features of proteins. Proteins 34, 82–95.

Ulmer, T.S., Ramirez, B.E., Delaglio, F., and Bax, A. (2003). Evaluation of backbone proton positions and dynamics in a small protein by liquid crystal NMR spectroscopy. J. Am. Chem. Soc. 125, 9179–9191.

van Rossum, B.J., Castellani, F., Rehbein, K., Pauli, J., and Oschkinat, H. (2001). Assignment of the nonexchanging protons of the α-spectrin SH3 domain by two- and three-dimensional ^{1}H-^{13}C solid-state magic-angle spinning NMR and comparison of solution and solid-state proton chemical shifts. ChemBioChem 2, 906–914.

van Rossum, B.J., Castellani, F., Pauli, J., Rehbein, K., Hollander, J., de Groot, H.J.M., and Oschkinat, H. (2003). Assignment of amide proton signals by combined evaluation of HN, NN and HNCA MAS-NMR correlation spectra. J. Biomol. NMR 25, 217–223.

Williamson, M.P., and Asakura, T. (1993). Empirical comparisons of models for chemical-shift calculation in proteins. J. Magn. Reson. B 101, 63–71.

Wilton, D.J., Tunnicliffe, R.B., Kamatari, Y.O., Akasaka, K., and Williamson, M.P. (2008). Pressure-induced changes in the solution structure of the GB1 domain of protein G. Proteins 71, 1432–1440.

Wishart, D.S., Arndt, D., Berjanskii, M., Tang, P., Zhou, J., and Lin, G. (2008). CS23D: a web server for rapid protein structure generation using NMR chemical shifts and sequence data. Nucleic Acids Res. 36, W496–W502.

Xu, X.P., and Case, D.A. (2001). Automated prediction of ^{15}N, ^{13}Cα, ^{13}Cβ and ^{13}C$'$ chemical shifts in proteins using a density functional database. J. Biomol. NMR 21, 321–333.

Zech, S.G., Wand, A.J., and McDermott, A.E. (2005). Protein structure determination by high-resolution solid-state NMR spectroscopy: application to microcrystalline ubiquitin. J. Am. Chem. Soc. 127, 8618–8626.

Zhou, H., and Zhou, Y. (2002). Distance-scaled, finite ideal-gas reference state improves structure-derived potentials of mean force for structure selection and stability prediction. Protein Sci. 11, 2714–2726.

Zhou, D.H., Shea, J.J., Nieuwkoop, A.J., Franks, W.T., Wylie, B.J., Mullen, C., Sandoz, D., and Rienstra, C.M. (2007a). Solid-rate protein-structure determination with proton-detected triple-resonance 3D magic-angle-spinning NMR spectroscopy. Angew. Chem. Int. Ed. Engl. 46, 8380–8383.

Zhou, D.H., Shah, G., Cormos, M., Mullen, C., Sandoz, D., and Rienstra, C.M. (2007b). Proton-detected solid-state NMR spectroscopy of fully protonated proteins at 40 kHz magic-angle spinning. J. Am. Chem. Soc. 129, 11791–11801.